AMERICAN SOCIETY FOR MICROBIOLOGY | Journal of Virology®

VIRUS-CELL INTERACTIONS

A Polymorphism within the Internal Fusion Loop of the Ebola Virus Glycoprotein Modulates Host Cell Entry

Markus Hoffmann,[a] Lisa Crone,[a] Erik Dietzel,[b] Jennifer Paijo,[c] Mariana González-Hernández,[a] Inga Nehlmeier,[a] Ulrich Kalinke,[c] Stephan Becker,[b] Stefan Pöhlmann[a]

Infection Biology Unit, German Primate Center, Göttingen, Germany[a]; Institute of Virology, Philipps University Marburg, Marburg, Germany[b]; Institute for Experimental Infection Research, TWINCORE, Centre for Experimental and Clinical Infection Research, a joint venture between the Helmholtz Centre for Infection Research and the Hannover Medical School, Hannover, Germany[c]

ABSTRACT The large scale of the Ebola virus disease (EVD) outbreak in West Africa in 2013-2016 raised the question whether the host cell interactions of the responsible Ebola virus (EBOV) strain differed from those of other ebolaviruses. We previously reported that the glycoprotein (GP) of the virus circulating in West Africa in 2014 (EBOV2014) exhibited reduced ability to mediate entry into two nonhuman primate (NHP)-derived cell lines relative to the GP of EBOV1976. Here, we investigated the molecular determinants underlying the differential entry efficiency. We found that EBOV2014-GP-driven entry into diverse NHP-derived cell lines, as well as human monocyte-derived macrophages and dendritic cells, was reduced compared to EBOV1976-GP, although entry into most human- and all bat-derived cell lines tested was comparable. Moreover, EBOV2014 replication in NHP but not human cells was diminished relative to EBOV1976, suggesting that reduced cell entry translated into reduced viral spread. Mutagenic analysis of EBOV2014-GP and EBOV1976-GP revealed that an amino acid polymorphism in the receptor-binding domain, A82V, modulated entry efficiency in a cell line-independent manner and did not account for the reduced EBOV2014-GP-driven entry into NHP cells. In contrast, polymorphism T544I, located in the internal fusion loop in the GP2 subunit, was found to be responsible for the entry phenotype. These results suggest that position 544 is an important determinant of EBOV infectivity for both NHP and certain human target cells.

IMPORTANCE The Ebola virus disease outbreak in West Africa in 2013 entailed more than 10,000 deaths. The scale of the outbreak and its dramatic impact on human health raised the question whether the responsible virus was particularly adept at infecting human cells. Our study shows that an amino acid exchange, A82V, that was acquired during the epidemic and that was not observed in previously circulating viruses, increases viral entry into diverse target cells. In contrast, the epidemic virus showed a reduced ability to enter cells of nonhuman primates compared to the virus circulating in 1976, and a single amino acid exchange in the internal fusion loop of the viral glycoprotein was found to account for this phenotype.

KEYWORDS Ebola virus, glycoprotein, host cell entry, internal fusion loop

The family *Filoviridae* comprises three genera: *Ebolavirus*, *Marburgvirus*, and *Cuevavirus*. Ebola- and marburgviruses can cause severe and frequently fatal disease in humans. Members of the ebolavirus species *Zaire ebolavirus* (only member: Ebola virus [EBOV]), *Sudan ebolavirus* (only member: Sudan virus), and *Bundibugyo ebolavirus* (only member: Bundibugyo virus) were associated with outbreaks of ebolavirus disease (EVD)

Received 31 January 2017 **Accepted** 15 February 2017

Accepted manuscript posted online 22 February 2017

Citation Hoffmann M, Crone L, Dietzel E, Paijo J, González-Hernández M, Nehlmeier I, Kalinke U, Becker S, Pöhlmann S. 2017. A polymorphism within the internal fusion loop of the Ebola virus glycoprotein modulates host cell entry. J Virol 91:e00177-17. https://doi.org/10.1128/JVI.00177-17.

Editor Terence S. Dermody, University of Pittsburgh School of Medicine

Address correspondence to Markus Hoffmann, mhoffmann@dpz.eu, or Stefan Pöhlmann, spoehlmann@dpz.eu.

occurring in remote areas in Central Africa. In 2013, this outbreak pattern changed: EBOV emerged for the first time in West Africa and the outbreak evolved for the first time into an epidemic. The epidemic spread of EBOV in Western Africa had dramatic consequences. More than 30,000 people were infected, and more than 10,000 of EVD patients died from the disease (1). Moreover, the epidemic included secondary cases in the United States and Spain (1, 2), demonstrating that EVD poses a global public health threat. The efficient spread of the epidemic EBOV (strain Makona) raised the question whether this virus was better adapted to infection of humans than previously circulating viruses, potentially due to more efficient interactions with human cells (3).

The EBOV glycoprotein (GP) mediates viral binding and entry into target cells (4). For this, the surface unit, GP1, of GP binds to cellular receptors, while the transmembrane unit, GP2, fuses the viral envelope with an endosomal membrane (5, 6). Binding to receptors is dependent on the integrity of a receptor-binding domain (RBD) within GP1, which interacts with the endosomal protein NPC1 (7, 8) upon proteolytic processing of GP by the endo-/lysosomal proteases cathepsin B and cathepsin L (9, 10). The membrane fusion reaction depends on the integrity of an internal fusion loop in GP2, which is located between the N terminus and the transmembrane domain and inserts into the target cell membrane during GP-driven membrane fusion (11–13). Several recent studies reported that the GP of the virus circulating in West Africa had acquired an amino acid exchange, A82V, in the RBD during the course of the epidemic, which increased viral infectivity (14–16), and one study provided evidence that A82V may be associated with augmented viral load and mortality (14). We previously compared entry driven by the GP of the virus circulating in West Africa in 2014 (EBOV2014) and the GP of the virus responsible for an EVD outbreak in Zaire in 1976 (EBOV1976, Mayinga strain) and found no obvious differences (17, 18). The only exception was entry into two cell lines derived from nonhuman primates (NHP), which was reduced for EBOV2014-GP compared to EBOV1976-GP (17, 18).

Here, we investigated why EBOV2014-GP mediated entry into NHP-derived cell lines with reduced efficiency compared to EBOV1976. We found that this entry phenotype was due to an amino acid polymorphism in the internal fusion loop, T544I. In contrast, mutation A82V enhanced entry independent of the origin of the cell line tested and was not responsible for the reduced EBOV2014-GP-mediated entry into NHP cells.

RESULTS

Attenuated growth of rEBOV2014 compared to rEBOV1976 in cells of African green monkey but not human origin. We previously observed that EBOV2014-GP mediated entry into two NHP cell lines with reduced efficiency compared to EBOV1976-GP, whereas entry into human target cell lines was comparable (17, 18). We first sought to clarify whether the differential entry efficiency translated into differential growth kinetics of the authentic EBOV. For this, we generated infectious EBOV1976 and EBOV2014 using reverse-genetics systems and assessed viral growth in Huh-7 cells (human origin) and Vero E6 cells (African green monkey origin). Determination of viral titers in culture supernatants revealed that both viruses grew with comparable efficiency in Huh-7 cells, whereas the growth of rEBOV1976 in Vero E6 cells was more efficient compared to its pendant from 2014 (Fig. 1). These observations and our published results (17, 18) suggest that the specific infectivity of EBOV2014 for NHP cell lines is reduced compared to human cells and that this defect is due to reduced host cell entry. Therefore, we focused our study on the question which determinants in EBOV2014-GP are responsible for the reduced entry into NHP-derived target cells.

EBOV2014-GP-driven entry into nonhuman primate cell lines is reduced compared to EBOV1976-GP. Within our previous analyses we had identified two NHP-derived cell lines (Vero and COS-7) with markedly reduced susceptibility to EBOV2014-GP-driven transduction (17, 18). Therefore, we next sought to determine whether the compromised ability of EBOV2014-GP to mediate entry into NHP cells was cell line dependent or a general phenotype. In addition, we compared EBOV1976-GP and EBOV2014-GP-driven entry into several cell lines of fruit bat (the natural reservoir)

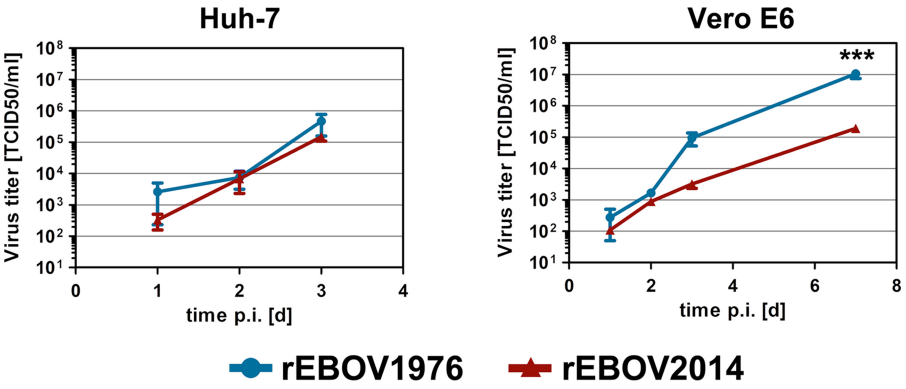

FIG 1 Reduced entry and replication of EBOV2014 in African green monkey but not human cells compared to EBOV1976. Human (Huh-7) and African green monkey (Vero E6) cells were infected with replication-competent, recombinant EBOV1976 (blue) or EBOV2014 (red), and samples were collected every 24 h for 3 (Huh-7) to 7 (Vero E6) days. Viral growth curves with mean titers of three individual experiments are shown. Error bars indicate standard errors of the mean. A two-way analysis of variance with the Bonferroni posttest was used to assess statistical significance (***, $P < 0.001$). (The data for EBOV2014 have previously been shown by Dietzel et al. in Fig. 5C in reference 16.)

and human origin. For this, we used rhabdoviral vectors pseudotyped with either EBOV1976-GP or EBOV2014-GP. The two glycoproteins mediated entry into two (HEK-293T and Huh-7) out of three human cell lines and all fruit bat cell lines (HypNi/1.1, RoNi/7, and EpoNi/22.1) with comparable efficiency (Fig. 2A). In contrast, for the human osteosarcoma cell line (HOS) and for human monocyte-derived macrophages (Mϕs) and dendritic cells, transduction mediated by EBOV2014-GP was less efficient than that measured for EBOV1976-GP (Fig. 2). Moreover, EBOV2014-GP-mediated entry into all NHP cell lines tested (LLC-MK2, sMAGI, Vero, Vero E6, and COS-7) was less efficient compared to EBOV1976-GP (Fig. 2A). These results suggest that EBOV2014-GP mediates entry into NHP-derived cell lines, as well as monocyte-derived human macrophages and dendritic cells, less efficiently than EBOV1976-GP, although both GPs mediate comparable entry into most but not all human cell lines.

Polymorphism A82V does not account for reduced EBOV2014-GP-mediated entry into nonhuman primate cells. The GP of EBOV variant Makona from the West African EVD epidemic (EBOV2014-GP) differs from the EBOV-GP of the Mayinga variant from the 1976 outbreak in former Zaire (now Democratic Republic of Congo; EBOV1976-GP) by a total of 20 amino acid residues (19) (Fig. 3A; see also Table S1 in the supplemental material). Of particular interest is a single amino acid difference at position 82 within the RBD. Whereas the GP from all preepidemic EBOV, as well as all other filoviruses, harbor an alanine at position 82, most EBOV associated with the West African EVD epidemic possess a valine at this position (Fig. 4A). Moreover, it seems that EBOV2014 has evolved the valine at position 82 during the course of the epidemic, as indicated by the increased frequency of V82 during the course of the epidemic (Fig. 4B). Therefore, we investigated whether the presence of V82 accounts for the reduced ability of EBOV2014-GP to mediate entry into NHP cell lines.

To address whether valine at position 82 is responsible for the reduced EBOV2014-driven entry into NHP-derived target cells, we constructed mutant GPs carrying alanine or valine in the context of EBOV2014-GP and EBOV1976-GP, respectively (Fig. 3B). Western blot analysis revealed that the wild-type (wt) GPs and the GP mutants with alanine or valine at position 82 were incorporated into VSVpp with comparable efficiency (Fig. 3C). We observed a modest but not statistically significant increase in transduction efficiency by EBOV1976-GP for several cell lines (Huh-7, HOS, LLC-MK2, and HypNi/1.1) when the EBOV2014-GP-specific valine was present at position 82 (Fig. 4C). However, the increased transduction efficiency was not specific for NHP-derived target cell lines. Vice versa, when the valine in EBOV2014-GP was changed to the EBOV1976-GP-specific alanine, transduction efficiency was reduced for all but two

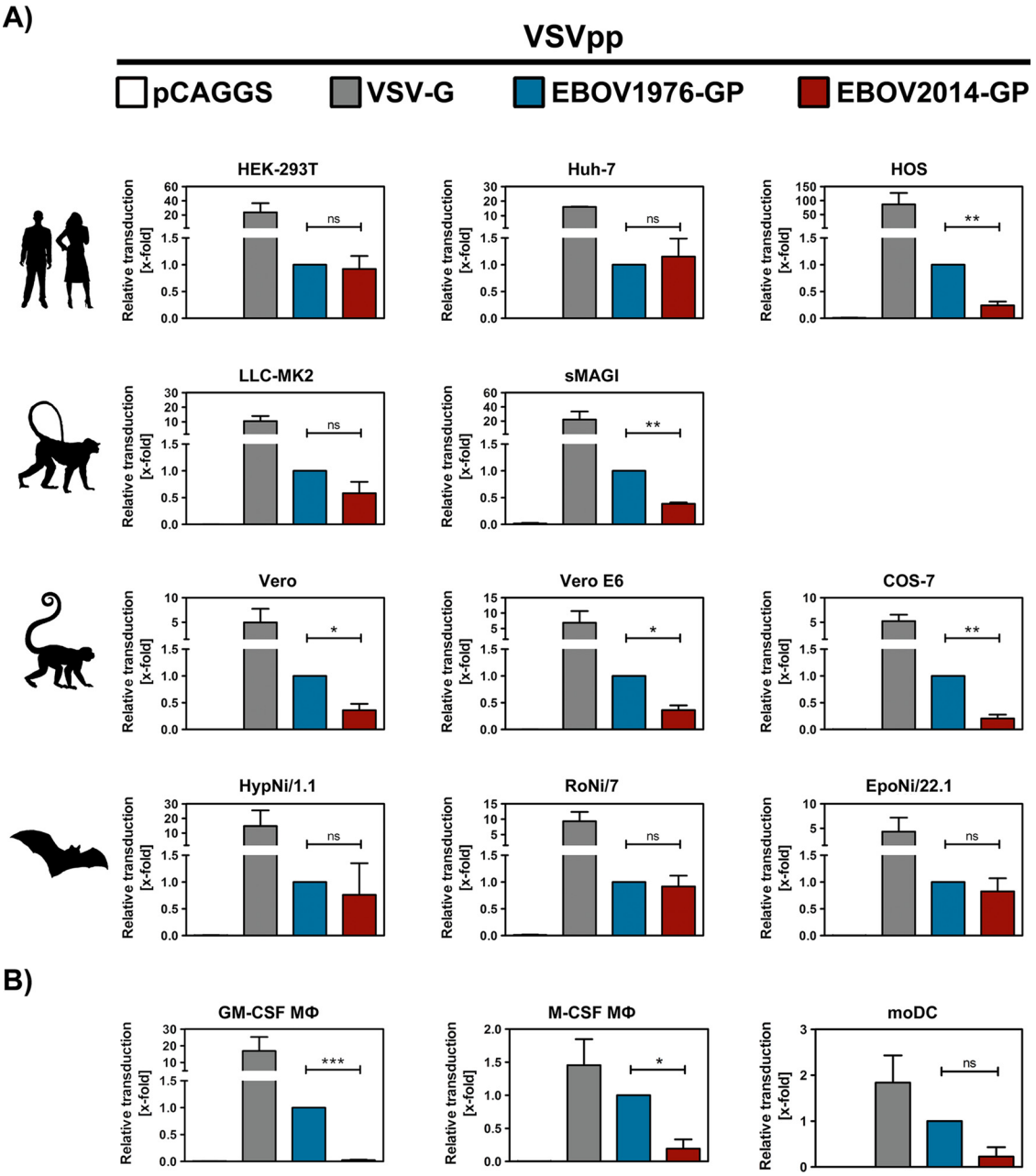

FIG 2 EBOV2014-GP-mediated entry into nonhuman primate cell lines, human HOS cells, and human monocyte-derived macrophages and dendritic cells is less efficient compared to EBOV1976-GP. Replication-deficient VSV encoding firefly luciferase was pseudotyped with VSV-G (positive control, gray), EBOV1976-GP (blue), EBOV2014-GP (red), or no glycoprotein (pCAGGS, negative control, white) and inoculated onto different mammalian cell lines of human (HEK-293T, Huh-7, HOS), rhesus macaque (LLC-MK2, sMAGI), African green monkey (Vero, Vero E6, COS-7) or fruit bat (HypNi/1.1, RoNi/7, and EpoNi/22.1) origin (A) or onto monocyte-derived macrophages (Mϕs) and dendritic cells (moDCs) (B). At 18 h postinoculation, the transduction efficiency was quantified by measuring firefly luciferase activity in cell lysates. The average of at least three independent experiments (with separate pseudotype preparations) is shown for panel A, while for panel B the monocyte-derived macrophages and dendritic cells from three individual donors were analyzed with one pseudotype preparation that has been previously tested on HEK-293T cells for comparable transduction efficiency. For all experiments, transduction mediated by EBOV1976-GP was set as one and x-fold changes are indicated. Error bars indicate the standard errors of the mean. A paired, two-tailed Student *t* test was used to assess statistical significance (*, $P < 0.05$; **, $P < 0.01$; ***, $P < 0.001$; ns, no significance).

(sMAGI and HypNi/1.1) of the cell lines tested, and the effects observed for Vero and Vero E6 were statistically significant (Fig. 4C). These results suggest that a valine at position 82 can increase entry into target cells of human and NHP origin, which is largely compatible with recent findings (14–16), although a decrease in bat cell tropism

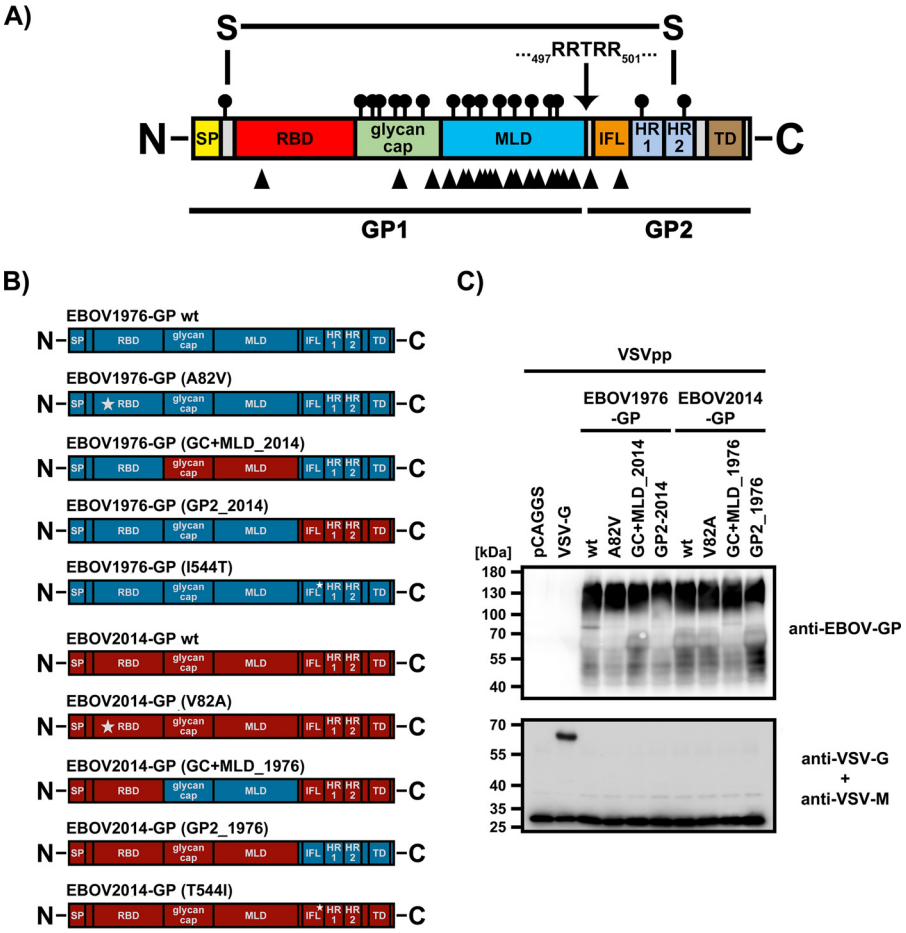

FIG 3 EBOV-GP mutants analyzed. (A) Domain organization of EBOV-GP. The signal peptide (SP; yellow), receptor binding domain (RBD; red), glycan cap (green), mucin-like domain (MLD; blue), internal fusion loop (IFL; orange), heptad repeats 1 and 2 (HR1 and HR2; light blue), transmembrane domain (TD; brown) are indicated. Signals for N-glycosylation (circles with lines) and amino acid polymorphisms between EBOV1976-GP and EBOV2014-GP (black arrowheads) are marked above and below the GP, respectively. The furin cleavage site located between GP1 and GP2 is indicated by an arrow, and the sequence is shown. (B) EBOV-GP mutants analyzed. Substitutions of single amino acids are indicated by stars and gave rise to mutants EBOV1976-GP (A82V), EBOV2014-GP (V82A), EBOV1976-GP (I544T), and EBOV2014-GP (T544I). Domains or subunits were exchanged in mutants EBOV1976-GP (GC+MLD_2014), EBOV2014-GP (GC+MLD_1976), EBOV1976-GP (GP2_2014), and EBOV2014-GP (GP2_1976). Domains or subunits derived from EBOV1976-GP are indicated in blue, and their counterparts from EBOV2014-GP are shown in red. (C) Equal volumes of pseudotypes bearing the indicated GPs were pelleted through a 20% sucrose cushion and subjected to Western blot analysis. The GP was detected using an EBOV-GP-specific rabbit antiserum and peroxidase-coupled, rabbit-specific secondary antibodies. In addition, VSV-G and VSV-M were visualized using monoclonal primary antibodies and peroxidase-coupled, mouse-specific secondary antibodies. The numbers on the left indicate molecular masses in kilodaltons (kDa). Similar results were obtained in a separate experiment.

(15) could not be observed. However, the effects observed were relatively modest, frequently not statistically significant and did not account for the marked difference between EBOV1974-GP- and EBOV2014-GP-mediated entry into NHP cells.

The GP2 subunit accounts for the reduced EBOV2014-GP-driven entry into nonhuman primate cells. We next sought to determine which of the amino acid polymorphisms other than V82A in EBOV2014-GP relative to EBOV1974-GP accounted for the reduced entry into NHP cell lines and certain human cell lines. Of a total of 20 amino acid differences between EBOV1976-GP and EBOV2014-GP, 18 reside within the GP1 subunit (Fig. 3A and see Table S1 in the supplemental material), with one exchange (V82A) residing in the RBD, two in the glycan cap and 15 in the mucin-like domain (MLD) (Fig. 3A and Table S1). The remaining two polymorphisms are located in the GP2 subunit with one being located between the furin cleavage site and the N terminus of

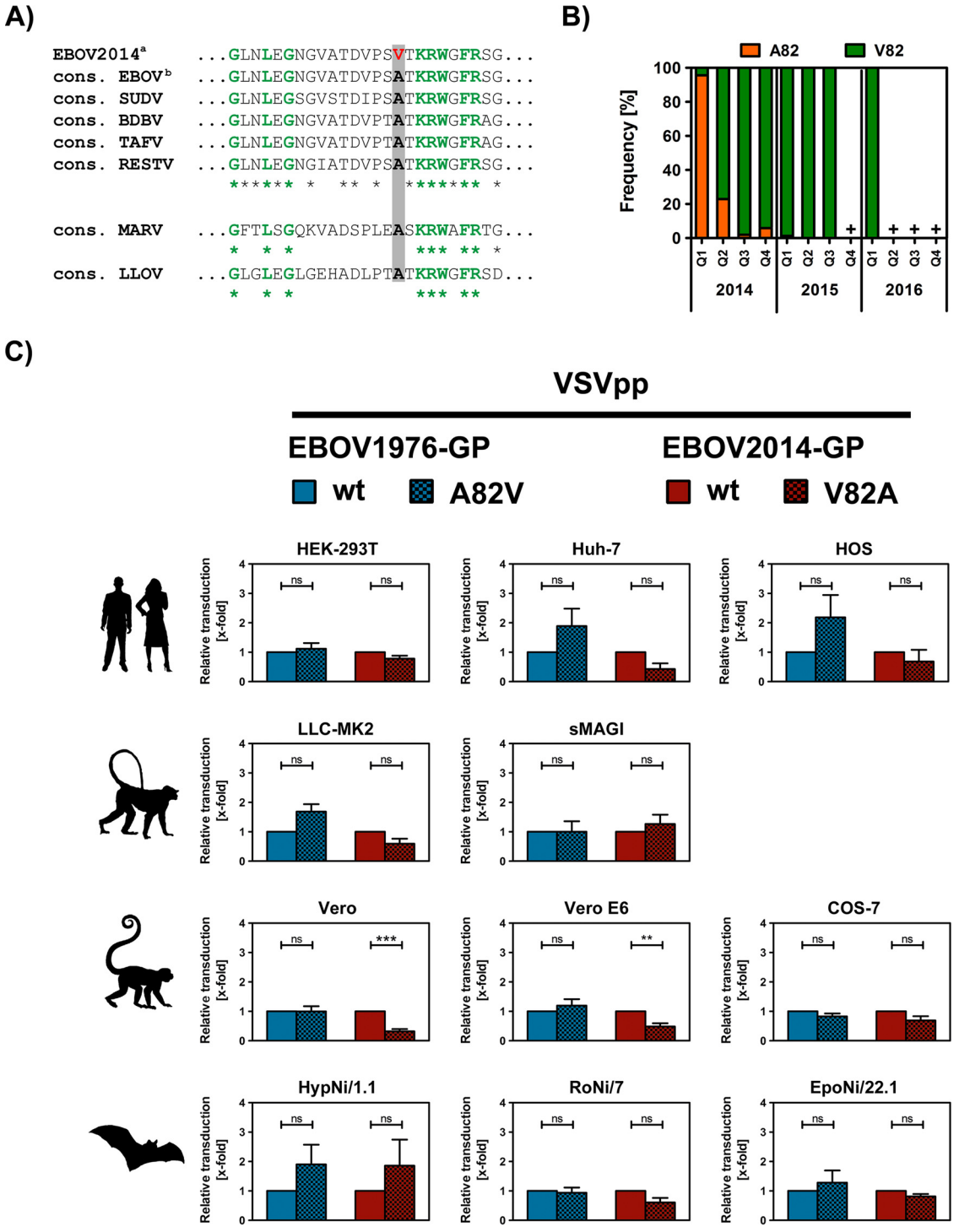

FIG 4 The A82V polymorphism in the receptor binding domain of EBOV2014-GP does not account for the reduced entry into nonhuman primate cells. (A) Alignment of amino acid residues 67 to 91 of EBOV2014-GP (superscript a, KM233105.1) and consensus sequences for all available GP sequences of EBOV not linked to the West African epidemic (superscript b), Sudan virus (SUDV), Bundibugyo virus (BDBV), Taï Forest virus (TAFV), Reston virus (RESTV), Marburg virus (MARV), and Lloviu virus (LLOV). Conserved amino acid residues among EBOV are indicated with an asterisk and amino acid residues present among all filoviruses are additionally highlighted in green. At amino acid position 82 (numbering according to EBOV-GP, gray box), the GP sequences of some EBOV2014 isolates contain a valine (red, bold), while all other filoviruses possess an alanine at that position (black, bold). (B) Frequencies of A82 and V82 among 970 GP sequences from viruses sampled during the West African EVD epidemic are graphed for the different quartiles (Q1 to Q4) between 2014 and 2016. Pluses indicate intervals where no EBOV isolate was reported. 97.7% of the sequences stem from the three West African countries mainly hit by the epidemic, Guinea (22.6%), Liberia (19.6%), and Sierra Leone (55.5%). (C) Rhabdoviral pseudotypes harboring wild-type (wt) or mutant (A82V, V82A) EBOV1976-GP and EBOV2014-GP were inoculated onto different mammalian cell lines. At 18 h postinoculation, transduction efficiency was quantified by measuring firefly luciferase activity in cell

(Continued on next page)

the internal fusion loop (position 503) and one being present within the internal fusion loop (position 544) (Fig. 3A; see also Fig. 6A and Table S1).

To address the role of these amino acid differences in the reduced EBOV2014-GP-mediated entry into NHP and certain human target cells, we constructed GP chimeras between EBOV1976-GP and EBOV2014-GP by either swapping the GP2 subunits or by exchanging the glycan cap jointly with the MLD (Fig. 3B). As for the mutants with exchanges at position 82, the chimeric GPs were incorporated into rhabdoviral vectors with an efficiency similar to that of wild-type GP (Fig. 3C). The exchange of glycan cap jointly with the MLD did not appreciably alter entry efficiency compared to the wt GPs (Fig. 5). In contrast, introduction of the GP2 subunit of EBOV1976-GP into EBOV2014-GP increased entry efficiency, while the converse effect was observed when the GP2 subunit of EBOV2014-GP was introduced into EBOV1976-GP (Fig. 5). Importantly, these effects were most pronounced for those cell lines that in previous experiments were less susceptible to transduction driven by wild-type EBOV2014-GP compared to EBOV1976-GP, i.e., all NHP-derived cell lines and the human osteosarcoma cell line HOS (Fig. 2A). These observations suggest that the reduced EBOV2014-GP-driven entry into NHP and certain human target cells compared to EBOV1976-GP is due to amino acid exchanges located in the GP2 subunit.

Polymorphism I544T located in the internal fusion loop is responsible for the compromised EBOV2014-GP-driven entry into nonhuman primate cells. The GP2 subunits of EBOV1976 and EBOV2014 harbor amino acid exchanges at positions 503 (alanine in EBOV1976-GP, valine in EBOV2014-GP) and 544 (isoleucine in EBOV1976-GP, threonine in EBOV2014-GP), respectively (Fig. 6A), and analysis of preepidemic EBOV-GP sequences ($n = 66$) revealed that 62.1% possess T544, while 37.9% have I544 (Fig. 6B). This raised the question which exchange contributed to the reduced EBOV2014-GP-driven entry into NHP and certain human target cells. A previous study reported that I544 is important for membrane fusion and that exchange I544A severely reduced both lipid mixing and GP-driven entry (12). Therefore, we focused our analysis on this position. Mutation of T544I in EBOV2014-GP (mutant EBOV2014-GP [T544I]) significantly increased transduction of COS-7 cells (Fig. 6C), for which we previously observed reduced entry driven by EBOV2014-GP relative to EBOV1976-GP (Fig. 2A). Conversely, exchange I544T in EBOV1976-GP (mutant EBOV1976-GP [I544T]) reduced entry efficiency (Fig. 6C). Finally, we sought to determine whether the results obtained with rhabdoviral pseudotypes can be recapitulated with EBOV-like particles. For this, we made use of a previously published virus-like particle (VLP) system based on EBOV-VP30 fused to luciferase (16). As observed for pseudotypes, substitution I544T reduced entry driven by EBOV1976-GP, while the reverse exchange increased EBOV2014-GP-driven entry (Fig. 6D). Collectively, these results demonstrate that a single amino acid polymorphism, I544T, in the GP2 subunit of EBOV2014-GP is responsible for the reduced ability of EBOV2014-GP to mediate entry into NHP and certain human cells compared to EBOV1976-GP.

DISCUSSION

The West African EVD epidemic had a dramatic impact on human health (1). Elucidating whether amino acid polymorphisms in the virus responsible for the epidemic endowed this virus with increased infectivity and transmissibility is key to understanding the course of the epidemic. The present study shows that V82 in EBOV2014 increases entry into target cells from diverse organs and species. In contrast, T544 reduced entry into NHP-derived cell lines and one human cell line and most likely accounts for the reduced ability of EBOV2014 to grow in NHP cells and to cause disease in experimentally infected NHP (20) compared to EBOV1976.

FIG 4 Legend (Continued)

lysates. For each pair (EBOV1976-GP wt/EBOV1976-GP [A82V] and EBOV2014-GP wt/EBOV2014-GP [V82A]), the average of at least three independent experiments (with separate pseudotype preparations) is shown. Results were normalized against transduction mediated by the respective wt GP (set as one) and are shown as x-fold changes. Error bars indicate the standard errors of the mean. A paired, two-tailed Student *t* test was used to assess statistical significance (*, $P < 0.05$; **, $P < 0.01$; ***, $P < 0.001$; ns, no significance).

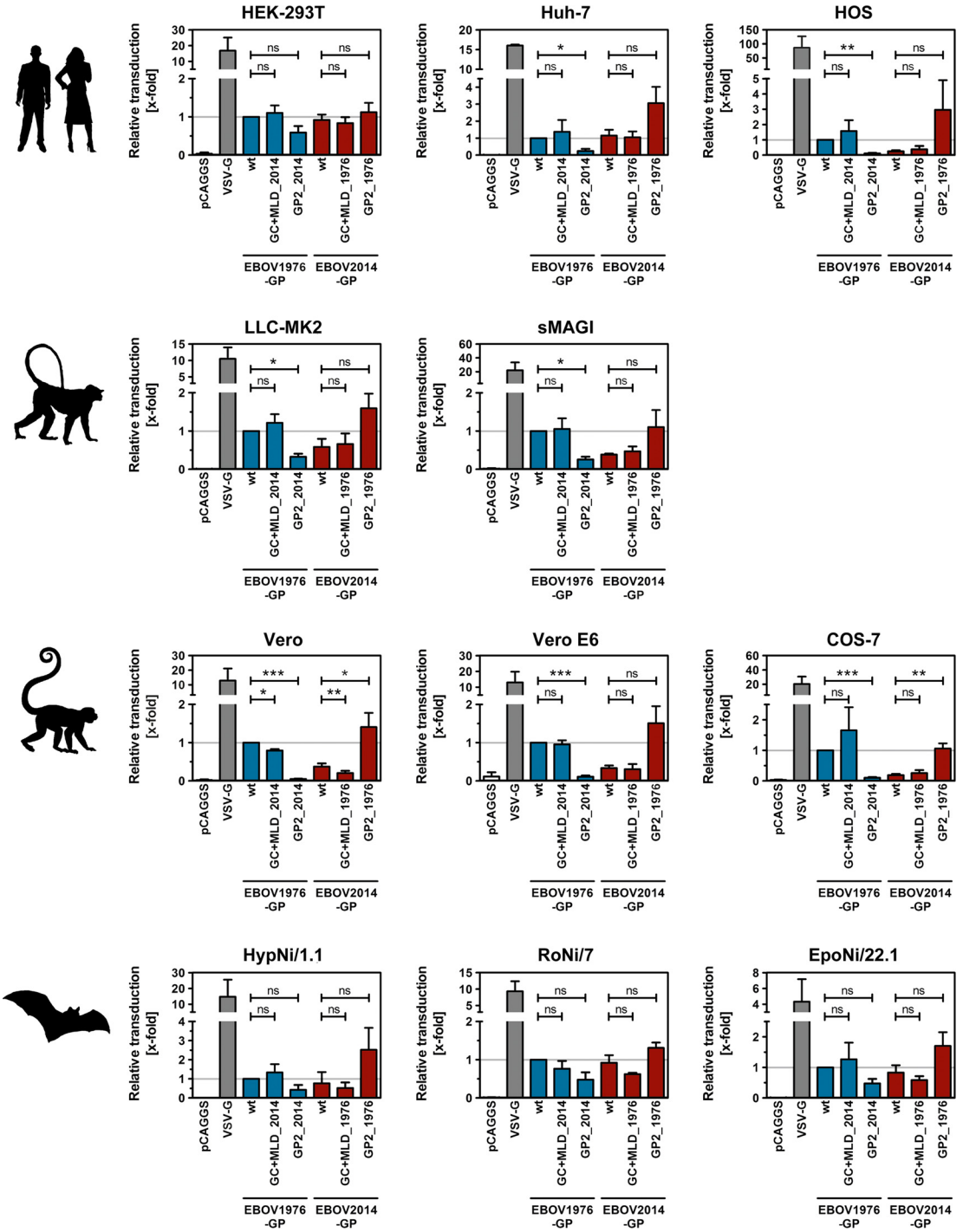

FIG 5 Determinants in the GP2 subunits account for the reduced EBOV2014-GP-mediated entry into nonhuman primate cells. Rhabdoviral pseudotypes harboring no glycoprotein (pCAGGS, negative control, white), VSV-G (positive control, gray), EBOV1976-GP wt (blue), EBOV2014-GP (red), and the indicated chimeras were inoculated onto different mammalian cell lines. At 18 h postinoculation, the transduction efficiency was quantified by measuring the firefly luciferase activity in cell lysates. The averages of three independent experiments (with separate pseudotype preparations) are shown. Results were normalized against transduction mediated by EBOV1976-GP wt (set as one) and are shown as x-fold changes. Error bars indicate the standard errors of the mean. A paired, two-tailed Student *t* test was used to assess statistical significance (*, $P < 0.05$; **, $P < 0.01$; ***, $P < 0.001$; ns, no significance).

Our results show that EBOV2014-GP mediated entry into diverse NHP-derived cell lines with reduced efficiency compared to EBOV1976-GP, although entry into most human and bat-derived cell lines was comparable. We first speculated that this might be due to reduced ability of EBOV2014-GP to use NHP-derived factors such as NPC1 for

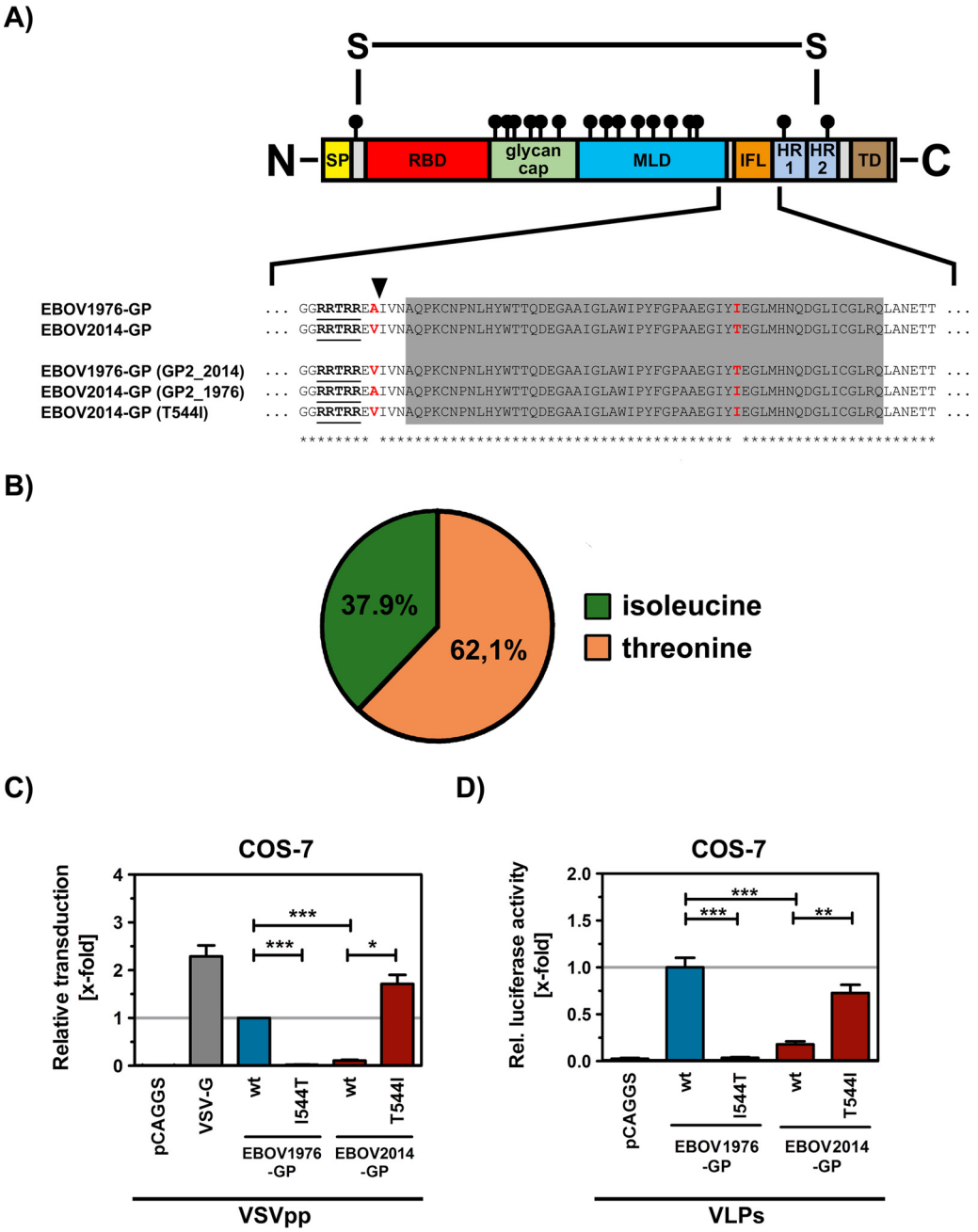

FIG 6 A single polymorphism, T544I, in GP2 accounts for the differential ability of EBOV2014-GP and EBOV1976-GP to drive entry into nonhuman primate cells. (A) The sequences spanning the border between GP1 and GP2 were aligned for the wt and mutant GPs analyzed. Conserved amino acid residues are marked with asterisks, while residues that differ between two GPs are indicated by bold, red letters. Amino acid residues of the internal fusion loop (IFL) are highlighted by a gray box. (B) All complete EBOV-GP sequences available at NCBI database that were not linked to the West African epidemic ($n = 66$) were analyzed for the amino acid present at position 544. The relative distribution of threonine (orange) and isoleucine (green) is shown. (C) Rhabdoviral pseudotypes harboring wild-type (wt) EBOV1976-GP, EBOV1976-GP (I544T) (both blue), wt EBOV2014-GP, or EBOV2014-GP (T544I) (both red) were inoculated onto COS-7 cells. Pseudotypes that contained no glycoprotein (pCAGGS, white) or VSV-G (gray) served as negative and positive controls, respectively. At 18 h postinoculation, transduction efficiency was quantified by measuring firefly luciferase activity in cell lysates. The average of three independent experiments (with separate pseudotype preparations) is shown. Results were normalized against transduction mediated by EBOV1976-GP wt (set as one) and are shown as x-fold changes. Error bars indicate the standard error of the mean. (D) EBOV-based VLPs harboring either no glycoprotein (white, negative control), wt EBOV1976-GP, EBOV1976-GP (I544T), wt EBOV2014-GP, or EBOV2014-GP (T544I) were inoculated onto COS-7 cells. At 3 h postinoculation, the firefly luciferase activity in cell lysates was quantified, corrected for background activity (measured in cells inoculated with pseudotypes not bearing a glycoprotein), and normalized against luciferase activity of VLPs used for inoculation (input factor). The results of a representative experiment carried out with quadruplicate samples are shown. Error bars indicate standard deviations. Similar results were obtained in two separate experiments performed with independent VLP preparations. Paired (pseudotypes) and unpaired (VLPs) two-tailed Student *t* tests were used to assess statistical significance (*, $P < 0.05$; **, $P < 0.01$; ***, $P < 0.001$; ns, no significance).

cell entry. However, preliminary data indicated that EBOV2014-GP could use human and NHP-derived NPC1 with similar efficiency for entry into NPC1-transfected cells (not shown), and subsequent mutagenic analysis of GP pointed toward a central contribution of the internal fusion loop, as discussed below. Notably, reduced EBOV2014-GP-driven entry (compared to EBOV1976-GP) was also observed with human HOS cells and, more importantly, human macrophages and dendritic cells, which constitute important viral targets. Thus, the factors limiting EBOV2014-GP-driven entry into NHP cells might also be operative in certain human cells, in keeping with the reduced virulence of EBOV2014 in a humanized mouse model compared to EBOV1976 (21). Finally, it is noteworthy that reduced EBOV2014-GP-driven entry into NHP cells relative to EBOV1976-GP was paralleled by reduced replication of authentic EBOV2014 in NHP cells. This finding is compatible with the observation that macaques infected with EBOV2014 show delayed disease progression compared to animals infected with EBOV1976 (20), and one can speculate that reduced infection of macrophages and dendritic cells, which plays a critical role in viral pathogenesis (22), might have contributed to differences in pathogenicity. Collectively, our results suggested that EBOV2014-GP had a specific defect in entry into NHP and certain human cells which translated into reduced viral replication, raising the question which determinants in GP were responsible for this phenotype.

We first focused our attention on position 82 since polymorphism A82V within EBOV2014-GP was not found in any previously characterized EBOV-GP. Functional analysis revealed that this position modulated entry efficiency. Thus, exchanging valine 82 with alanine (V82A) reduced EBOV2014-GP into human, NHP, and bat-derived cell lines, whereas the reverse exchange increased cell entry driven by EBOV1976-GP. Since the effects observed were modest, species independent, and frequently not statistically significant, they could not account for the differential ability of EBOV2014-GP and EBOV1976-GP to mediate entry into NHP cells. A previous study showed that A82V was under positive selection during the West African EVD epidemic (23), and several recent studies have demonstrated that the acquisition of A82V was associated with increased viral entry into and/or replication in human cells (14–16, 23). In addition, Diehl et al. reported an association of A82V with increased viral load and mortality, but only the latter association was statistically significant (14). In general, our results are in accord with these observations. However, we did not observe that mutation A82V reduced entry into bat-derived cell lines, as suggested by Urbanowicz et al. (15). Similarly, our study does not support the notion that reduced ability of EBOV2014-GP to use NPC1 of bat origin for entry translates into diminished specific infectivity for bat-derived cell lines. The reasons for these differential observations are at present unclear but might relate to use of different pseudotyping systems (Urbanowicz et al. used retroviral vectors, we used vesicular stomatitis virus-based pseudotypes) and the sensitivity of signal detection, given the moderate nature of the effects observed (~2-fold differences between parental Ma C15 and B1 were reported previously [15]).

Analysis of chimeric GPs suggested that differences in GP2 accounted for the differential ability of EBOV2014-GP and EBOV1976-GP to enter NHP cells and polymorphism T544I was found to be responsible for this entry phenotype. Position 544 resides within the internal fusion loop and was previously reported to be essential for efficient membrane fusion and entry (12). One can speculate that the internal fusion loop present in EBOV2014-GP is less well able to support fusion with NHP cell membranes compared to its counterpart from EBOV1976-GP, potentially due to less efficient insertion into the target cell membrane resulting from a suboptimal formation of the fusogenic hydrophobic surface. Further studies are required to define the mechanism. We focused on the question which GPs harbor polymorphism T544I, which was found by the present study to be associated with increased entry into NHP and certain human cells. Inspection of 66 EBOV-GP sequences not linked to the West African epidemic revealed that 25 (37.9%, Fig. 6B) contained I544 (see Table S3 in the supplemental material). For 21 of these 25 sequences, additional information was available and revealed that they were obtained from EBOV that were extensively passaged in cell

culture ($n = 19$) or guinea pigs ($n = 1$) or that were successively passaged in cell culture, monkeys, and again cell culture ($n = 1$). For passaging in cell culture, NHP-derived Vero E6 cells were frequently used. Next, we analyzed 1,094 GP sequences associated with the West African EVD epidemic and found that 10 (0.91%) contained an isoleucine at position 544. Six of these ten sequences were derived from EBOV that had been passaged in cell culture prior to sequencing (see Table S4 in the supplemental material). Finally, two GenBank entries are noteworthy that were made for the same virus before (Ebola virus/H.sapiens-wt/GIN/2014/Makona-C05 [Makona-C05_wt]; KJ660348.2) and after passaging ($n = 3$) in Vero E6 cells (Ebola virus/H.sapiens-tc/GIN/2014/Makona-C05 [Makona-C05_tc]; KX000398.1): the nonpassaged virus harbored threonine at position 544, while the passaged virus contained an isoleucine. Collectively, these results suggest that I544 is a cell culture adaptation. However, we cannot exclude that EBOV harboring I544 is present in patients at very low frequency and becomes dominant upon viral propagation in cell culture.

In summary, our results indicate that EBOV from infected humans harbor T544, although exchange T544I markedly increases viral entry into NHP-derived cell lines and important human target cells, macrophages and dendritic cells. One can thus speculate that T544 may allow EBOV to evade immune pressure, for instance, by inhibiting STING activation (24) or by reducing T cell responses against the surrounding epitope (25), and that this trait comes at the cost of reduced viral entry capacity.

MATERIALS AND METHODS

Cell culture. The following cell lines were used as targets for infection with replication-competent EBOV and for transduction with EBOV-GP-bearing pseudotypes and were maintained in Dulbecco modified Eagle medium (PAN-Biotech), supplemented with 10% fetal bovine serum (Biochrom) and antibiotics (penicillin-streptomycin; PAN-Biotech): HEK-293T, Huh-7, and HOS (all of human origin); LLC-MK-2 and CMMT-CD4-LTR-β-Gal (sMAGI; simian multinuclear activation of a galactosidase indicator cells [26]) (both of rhesus macaque origin); and Vero, Vero E6, and COS-7 (all of African green monkey origin). We also used fruit bat cell lines from three individual species, HypNi/1.1 (Hammer-headed fruit bat), RoNi/7 (Egyptian fruit bat), and EpoNi/22.1 (Buettikofer's epauletted fruit bat). All non-bat-derived cell lines were obtained from collaborators. The fruit bat cell lines were kindly provided by C. Drosten and M. A. Müller and have been described previously (27–31). All cell lines were grown in a humidified atmosphere at 37°C and 5% CO_2. For passaging and seeding, cells were detached by either resuspension in fresh culture medium (HEK-293T cells) or by the use of trypsin/EDTA (PAN-Biotech).

Plasmids. Expression plasmids for the glycoproteins of the EBOV from the 1976 outbreak in the Democratic Republic of Congo (Mayinga variant, EBOV1976-GP, GenBank accession number AF086833.2), Ebola virus/H.sapiens-wt/SLE/2014/Makona-G3838 of the West African EVD epidemic (Makona variant, EBOV2014-GP, GenBank accession number KM233105.1), and vesicular stomatitis virus (VSV; Indiana strain, VSV-G; GenBank accession number AJ318514.1) have been described previously (17, 18). To address the impact of the 20 amino acid polymorphisms between EBOV1976-GP and EBOV2014-GP (see Table S1 in the supplemental material), mutant GPs were generated in which single amino acid residues or functional domains between the two GPs were interchanged. For this, site-directed mutagenesis and overlap extension PCR were used. Specifically, we constructed chimeric GPs with swapped GP1/GP2 subunits (EBOV1976-GP [GP2_2014] and EBOV2014-GP [GP2_1976]) and GPs in which the glycan cap (GC) and the mucin-like domain (MLD) were interchanged (EBOV1976-GP [GC+MLD_2014] and EBOV2014-GP [GC+MLD_1976]). Moreover, EBOV1976-GP and EBOV2014-GP mutants were generated which harbored single amino acid exchanges at polymorphic sites within the RBD (EBOV1976-GP [A82V] and EBOV2014-GP [V82A]) or internal fusion loop (IFL; EBOV1976-GP [I544T] and EBOV2014-GP [T544I]). Plasmids for the generation of EBOV-like particles (VLPs) and for the rescue of replication-competent EBOV Mayinga (rEBOV1976) and Makona (prototype isolate, Makona C7, GenBank accession number KJ660347.2; rEBOV2014) variants have been described elsewhere (16, 32).

Infection of cell lines with replication-competent rEBOV1976 and rEBOV2014. All work with infectious EBOV was performed at the BSL-4 facility of the Institute of Virology, Philipps-University Marburg by trained personnel and in accordance with national regulations. Detailed protocols for the recovery of recombinant EBOV1976 and EBOV2014 from plasmids are described elsewhere (16, 33). To assess replication kinetics of rEBOV1976 and rEBOV2014 in Huh-7 and Vero E6 cells, cells were infected at a multiplicity of infection of 0.01. After 1 h at 37°C and 5% CO_2, the inoculum was removed, and fresh medium was added to the cells. Samples of the supernatant were collected at days 1, 2, 3, and 7 for Vero E6 cells and at days 1, 2, and 3 for Huh-7 cells. For the latter, sampling of later time points was not appropriate due to cytopathic effect. Clarified supernatant was titrated on Vero E6 cells and the 50% tissue culture infective dose/ml was calculated.

Isolation and differentiation of primary cells. Isolation, differentiation, and cultivation of monocyte-derived human macrophages (Mϕs) and monocyte-derived dendritic cells (moDCs) has been described previously (34). Briefly, $CD14^+$ monocytes were differentiated for 5 days in serum-free DC medium (CellGenix) in the presence of 80 U/ml GM-CSF (granulocyte macrophage-colony-stimulating factor;

CellGenix), 100 ng/ml M-CSF (macrophage-colony-stimulating factor; Miltenyi Biotec), or 1,000 U/ml GM-CSF plus 1,000 U/ml interleukin-4 (CellGenix) to derive GM-CSF Mϕs, M-CSF Mϕs, or moDCs, respectively.

Production of rhabdoviral pseudotypes. The production of rhabdoviral pseudotypes using a replication-deficient VSV vector has been described before in detail (18, 35). In brief, HEK-293T cells expressing the desired viral surface protein following calcium-phosphate precipitation were inoculated with VSV-G-transcomplemented VSV*ΔG-Luc (in the pseudotype genome, the genetic information for VSV-G has been replaced by two separate open reading frames, coding for enhanced green fluorescent protein and firefly luciferase [fLuc]). At 1 h postinfection, residual input virus was removed by washing the cells with phosphate-buffered saline (PBS) and adding a neutralizing antibody directed against VSV-G (I1, a mouse hybridoma supernatant from CRL-2700 [American Type Culture Collection]; 1:1,000). The cells were further incubated for 16 to 20 h, before the supernatants containing the VSV pseudotypes (VSVpp) were collected.

Analysis of GP incorporation into VSVpp by Western blotting. To assess whether chimeric and mutant GPs were incorporated into VSVpp with similar efficiency as wt EBOV1976-GP and EBOV2014-GP, equal volumes of pseudotype preparations were pelleted by high-speed centrifugation (17,000 $\times$ *g* for 2 h at 4°C) through a 20% sucrose cushion, resuspended in 30 μl of 2$\times$ sodium dodecyl sulfate (SDS)-containing lysis buffer (50 mM Tris [pH 6.8], 10% glycerol, 2% SDS, 5% β-mercaptoethanol, 0.1% bromophenol blue, 1 mM EDTA), and boiled for 20 min at 96°C before they were subjected to SDS-PAGE. After protein transfer to nitrocellulose membranes via Western blotting, membranes were blocked in PBS containing 5% skim milk for 2 h at room temperature. Finally, all samples were subjected to immunoblot analysis: the wild-type, mutant, and chimeric GP were detected using a GP1-specific rabbit serum (1:5,000) and a peroxidase-coupled anti-rabbit secondary antibody (Dianova; 1:5,000). To show that equal amounts of VSVpp were used and that GP-harboring VSVpp did not contain VSV-G, a separate membrane (obtained under the same conditions as described previously) was first incubated with a mixture of antibodies against VSV-M (matrix protein, raised in mice [KeraFast]; 1:1,000) and VSV-G (I1, mouse hybridoma supernatant from CRL-2700 [American Type Culture Collection]; 1:200) and then incubated with a peroxidase-linked anti-mouse secondary antibody (Dianova; 1:5,000). All antibodies were diluted in PBS containing 0.05% Tween 20 and 5% skim milk and after blocking, as well as between primary and secondary antibody incubation, membranes were washed three times with PBS containing 0.05% Tween 20. Signals of bound secondary antibodies were detected using a commercially available ECL kit (GE Healthcare) and visualized using the ChemoCam imaging system in combination with the Chemo StarProfessional software (Intas).

Transduction of cell lines with rhabdoviral pseudotypes and quantification of fLuc activity. Transduction experiments with mammalian cell lines were performed in quadruplicate samples with cells grown in 96-well plates. At 24 h postseeding, the cell culture medium was removed, and the cells were washed with PBS before VSVpp inoculation was performed for 1 h at 37°C and 5% CO_2. Afterward, the cells received fresh medium and were further incubated for 16 to 18 h at 37°C and 5% CO_2. To quantify the fLuc activity, the cell culture supernatant was aspirated, and the cells were washed with PBS before they were incubated with 50 μl of 1$\times$ luciferase cell culture lysis reagent (Promega) in PBS for 30 min at room temperature. The lysates were then transferred to a white, opaque-walled 96-well plate (Thermo Scientific) and fLuc activity was measured in a microplate reader, Plate Chameleon (Hidex), using the MicroWin2000 software (version 4.44; Mikrotek Laborsysteme, GmbH) and fLuc substrates from the luciferase assay system (Promega) or Beetle-Juice (PJK) kits. Transduction efficiency, represented by fLuc activity, is displayed as normalized values (x-fold or percentage from reference sample).

Transduction of monocyte-derived human macrophages and dendritic cells with rhabdoviral pseudotypes and quantification of fLuc activity. Transduction experiments with monocyte-derived human macrophages and dendritic cells were performed in triplicate samples. Cells were cultured and differentiated in 48-well plates for 5 days before transduction experiments were performed. For transduction, cells were pelleted by centrifugation (300 $\times$ *g*, 10 min) and, after removal of the supernatant, 500 μl of the rhabdoviral pseudotypes was added. After 16 to 18 h of incubation at 37°C and 5% CO_2, the cells were pelleted again and lysed in 200 μl of GloLysis buffer (Promega) for 30 min on ice. Then, 20 μl of cell lysates was transferred to a white, opaque-walled 96-well plate, and the fLuc activity was measured as described under "Transduction of cell lines with rhabdoviral pseudotypes and quantification of fLuc activity."

Production of EBOV-based VLPs and their use in entry studies. For the generation of EBOV-based VLPs, HEK-293T cells grown in T-75 cell culture flasks were transfected with 1 μg of EBOV-NP, 1 μg of EBOV-VP35, 8.3 μg of EBOV-L, 2 μg of EBOV-VP40, 12.5 μg of EBOV-VP30-Luc, and 2 μg of either EBOV1976-GP wt, EBOV1976-GP (I544T), EBOV2014-GP wt, EBOV2014-GP (T544I), or empty expression plasmid (pCAGGS, negative control) by calcium phosphate precipitation. At 16 h posttransfection, the cell culture supernatant was replaced by fresh culture medium, and the cells were further incubated for an additional 24 h before the supernatants were collected. The supernatants were clarified from debris by centrifugation (4,000 $\times$ *g*, 10 min) and concentrated using Vivaspin concentrators with a molecular mass cutoff of 30,000 kDa (Sartorius). Concentrated VLPs were adjusted to a final volume of 500 μl by addition of DMEM and inoculated onto confluent monolayers of COS-7 cells grown in 96-well plates. After an incubation period of 3 h at 37°C and 5% CO_2, the inoculum was removed, and the cells were washed with PBS before 50 μl of 1$\times$ luciferase cell culture lysis reagent (Promega) in PBS was added. Subsequently, the samples were processed as described above for the quantification of luciferase activity after pseudotype transduction.

Sequence analysis of filoviral glycoproteins. All GP sequences (see Table S2 in the supplemental material) were obtained from the National Center for Biotechnology Information database and alignments were performed on amino acid level using the ClustalOmega online tool (http://www.ebi.ac.uk/Tools/msa/clustalo/). Only complete GP sequences were included in the analysis. To generate consensus GP sequences for each genus within the *Filoviridae* family, sequences were first aligned and at positions with amino acid polymorphisms, the predominantly present amino acid residue was used. EBOV-GP sequences denoted "preepidemic" include those that are not linked to the West African EVD epidemic. If not mentioned in the NCBI database, detailed information on the passage background of selected EBOV was retrieved from publications linked to the respective sequence.

SUPPLEMENTAL MATERIAL

Supplemental material for this article may be found at https://doi.org/10.1128/JVI.00177-17.

SUPPLEMENTAL FILE 1, PDF file, 0.1 MB.

ACKNOWLEDGMENT

We thank Andrew Rambaut for helpful discussions.

REFERENCES

1. World Health Organization. 2016. Ebola situation report: 30 March 2016. World Health Organization, Geneva, Switzerland. http://apps.who.int/ebola/current-situation/ebola-situation-report-30-march-2016.
2. WHO Ebola Response Team. 2016. Ebola virus disease among male and female persons in West Africa. N Engl J Med 374:96–98. https://doi.org/10.1056/NEJMc1510305.
3. Simon-Loriere E, Faye O, Faye O, Koivogui L, Magassouba N, Keita S, Thiberge JM, Diancourt L, Bouchier C, Vandenbogaert M, Caro V, Fall G, Buchmann JP, Matranga CB, Sabeti PC, Manuguerra JC, Holmes EC, Sall AA. 2015. Distinct lineages of Ebola virus in Guinea during the 2014 West African epidemic. Nature 524:102–104. https://doi.org/10.1038/nature14612.
4. Hofmann-Winkler H, Kaup F, Pöhlmann S. 2012. Host cell factors in filovirus entry: novel players, new insights. Viruses 4:3336–3362. https://doi.org/10.3390/v4123336.
5. Weissenhorn W, Carfi A, Lee KH, Skehel JJ, Wiley DC. 1998. Crystal structure of the Ebola virus membrane fusion subunit, GP2, from the envelope glycoprotein ectodomain. Mol Cell 2:605–616. https://doi.org/10.1016/S1097-2765(00)80159-8.
6. Wang H, Shi Y, Song J, Qi J, Lu G, Yan J, Gao GF. 2016. Ebola viral glycoprotein bound to its endosomal receptor Niemann-Pick C1. Cell 164:258–268. https://doi.org/10.1016/j.cell.2015.12.044.
7. Carette JE, Raaben M, Wong AC, Herbert AS, Obernosterer G, Mulherkar N, Kuehne AI, Kranzusch PJ, Griffin AM, Ruthel G, Dal Cin P, Dye JM, Whelan SP, Chandran K, Brummelkamp TR. 2011. Ebola virus entry requires the cholesterol transporter Niemann-Pick C1. Nature 477:340–343. https://doi.org/10.1038/nature10348.
8. Cote M, Misasi J, Ren T, Bruchez A, Lee K, Filone CM, Hensley L, Li Q, Ory D, Chandran K, Cunningham J. 2011. Small molecule inhibitors reveal Niemann-Pick C1 is essential for Ebola virus infection. Nature 477:344–348. https://doi.org/10.1038/nature10380.
9. Chandran K, Sullivan NJ, Felbor U, Whelan SP, Cunningham JM. 2005. Endosomal proteolysis of the Ebola virus glycoprotein is necessary for infection. Science 308:1643–1645. https://doi.org/10.1126/science.1110656.
10. Schornberg K, Matsuyama S, Kabsch K, Delos S, Bouton A, White J. 2006. Role of endosomal cathepsins in entry mediated by the Ebola virus glycoprotein. J Virol 80:4174–4178. https://doi.org/10.1128/JVI.80.8.4174-4178.2006.
11. Ito H, Watanabe S, Sanchez A, Whitt MA, Kawaoka Y. 1999. Mutational analysis of the putative fusion domain of Ebola virus glycoprotein. J Virol 73:8907–8912.
12. Gregory SM, Larsson P, Nelson EA, Kasson PM, White JM, Tamm LK. 2014. Ebolavirus entry requires a compact hydrophobic fist at the tip of the fusion loop. J Virol 88:6636–6649. https://doi.org/10.1128/JVI.00396-14.
13. Gregory SM, Harada E, Liang B, Delos SE, White JM, Tamm LK. 2011. Structure and function of the complete internal fusion loop from Ebolavirus glycoprotein 2. Proc Natl Acad Sci U S A 108:11211–11216. https://doi.org/10.1073/pnas.1104760108.
14. Diehl WE, Lin AE, Grubaugh ND, Carvalho LM, Kim K, Kyawe PP, McCauley SM, Donnard E, Kucukural A, McDonel P, Schaffner SF, Garber M, Rambaut A, Andersen KG, Sabeti PC, Luban J. 2016. Ebola virus glycoprotein with increased infectivity dominated the 2013-2016 epidemic. Cell 167:1088–1098. https://doi.org/10.1016/j.cell.2016.10.014.
15. Urbanowicz RA, McClure CP, Sakuntabhai A, Sall AA, Kobinger G, Müller MA, Holmes EC, Rey FA, Simon-Loriere E, Ball JK. 2016. Human adaptation of Ebola virus during the West African outbreak. Cell 167:1079–1087. https://doi.org/10.1016/j.cell.2016.10.013.
16. Dietzel E, Schudt G, Krahling V, Matrosovich M, Becker S. 2017. Functional characterization of adaptive mutations during the West African Ebola virus outbreak. J Virol 91:e01913-16. https://doi.org/10.1128/JVI.01913-16.
17. Hofmann-Winkler H, Gnirss K, Wrensch F, Pöhlmann S. 2015. Comparative analysis of host cell entry of Ebola virus from Sierra Leone, 2014, and Zaire, 1976. J Infect Dis 212(Suppl 2):S172–S180. https://doi.org/10.1093/infdis/jiv101.
18. Hoffmann M, Gonzalez Hernandez M, Berger E, Marzi A, Pöhlmann S. 2016. The glycoproteins of all filovirus species use the same host factors for entry into bat and human cells but entry efficiency is species dependent. PLoS One 11:e0149651. https://doi.org/10.1371/journal.pone.0149651.
19. Khurana S, Fuentes S, Coyle EM, Ravichandran S, Davey RT, Jr, Beigel JH. 2016. Human antibody repertoire after VSV-Ebola vaccination identifies novel targets and virus-neutralizing IgM antibodies. Nat Med 22:1439–1447. https://doi.org/10.1038/nm.4201.
20. Marzi A, Feldmann F, Hanley PW, Scott DP, Gunther S, Feldmann H. 2015. Delayed disease progression in cynomolgus macaques infected with Ebola virus Makona strain. Emerg Infect Dis 21:1777–1783. https://doi.org/10.3201/eid2110.150259.
21. Bird BH, Spengler JR, Chakrabarti AK, Khristova ML, Sealy TK, Coleman-McCray JD, Martin BE, Dodd KA, Goldsmith CS, Sanders J, Zaki SR, Nichol ST, Spiropoulou CF. 2016. Humanized mouse model of Ebola virus disease mimics the immune responses in human disease. J Infect Dis 213:703–711. https://doi.org/10.1093/infdis/jiv538.
22. Rougeron V, Feldmann H, Grard G, Becker S, Leroy EM. 2015. Ebola and Marburg haemorrhagic fever. J Clin Virol 64:111–119. https://doi.org/10.1016/j.jcv.2015.01.014.
23. Ladner JT, Wiley MR, Mate S, Dudas G, Prieto K, Lovett S, Nagle ER, Beitzel B, Gilbert ML, Fakoli L, Diclaro JW, II, Schoepp RJ, Fair J, Kuhn JH, Hensley LE, Park DJ, Sabeti PC, Rambaut A, Sanchez-Lockhart M, Bolay FK, Kugelman JR, Palacios G. 2015. Evolution and spread of Ebola virus in Liberia, 2014-2015. Cell Host Microbe 18:659–669. https://doi.org/10.1016/j.chom.2015.11.008.
24. Holm CK, Rahbek SH, Gad HH, Bak RO, Jakobsen MR, Jiang Z, Hansen AL, Jensen SK, Sun C, Thomsen MK, Laustsen A, Nielsen CG, Severinsen K, Xiong Y, Burdette DL, Hornung V, Lebbink RJ, Duch M, Fitzgerald KA, Bahrami S, Mikkelsen JG, Hartmann R, Paludan SR. 2016. Influenza A virus targets a cGAS-independent STING pathway that controls enveloped RNA viruses. Nat Commun 7:10680. https://doi.org/10.1038/ncomms10680.
25. Olinger GG, Bailey MA, Dye JM, Bakken R, Kuehne A, Kondig J, Wilson J,

Hogan RJ, Hart MK. 2005. Protective cytotoxic T-cell responses induced by venezuelan equine encephalitis virus replicons expressing Ebola virus proteins. J Virol 79:14189–14196. https://doi.org/10.1128/JVI.79.22.14189-14196.2005.
26. Chackerian B, Haigwood NL, Overbaugh J. 1995. Characterization of a CD4-expressing macaque cell line that can detect virus after a single replication cycle and can be infected by diverse simian immunodeficiency virus isolates. Virology 213:386–394. https://doi.org/10.1006/viro.1995.0011.
27. Hoffmann M, Müller MA, Drexler JF, Glende J, Erdt M, Gutzkow T, Losemann C, Binger T, Deng H, Schwegmann-Wessels C, Esser KH, Drosten C, Herrler G. 2013. Differential sensitivity of bat cells to infection by enveloped RNA viruses: coronaviruses, paramyxoviruses, filoviruses, and influenza viruses. PLoS One 8:e72942. https://doi.org/10.1371/journal.pone.0072942.
28. Krüger N, Hoffmann M, Drexler JF, Muller MA, Corman VM, Drosten C, Herrler G. 2014. Attachment protein G of an African bat henipavirus is differentially restricted in chiropteran and nonchiropteran cells. J Virol 88:11973–11980. https://doi.org/10.1128/JVI.01561-14.
29. Kühl A, Hoffmann M, Müller MA, Munster VJ, Gnirss K, Kiene M, Tsegaye TS, Behrens G, Herrler G, Feldmann H, Drosten C, Pöhlmann S. 2011. Comparative analysis of Ebola virus glycoprotein interactions with human and bat cells. J Infect Dis 204(Suppl 3):S840–849. https://doi.org/10.1093/infdis/jir306.
30. Müller MA, Raj VS, Muth D, Meyer B, Kallies S, Smits SL, Wollny R, Bestebroer TM, Specht S, Suliman T, Zimmermann K, Binger T, Eckerle I, Tschapka M, Zaki AM, Osterhaus AD, Fouchier RA, Haagmans BL, Drosten C. 2012. Human coronavirus EMC does not require the SARS-coronavirus receptor and maintains broad replicative capability in mammalian cell lines. mBio 3:e00515-12. https://doi.org/10.1128/mBio.00515-12.
31. Biesold SE, Ritz D, Gloza-Rausch F, Wollny R, Drexler JF, Corman VM, Kalko EK, Oppong S, Drosten C, Müller MA. 2011. Type I interferon reaction to viral infection in interferon-competent, immortalized cell lines from the African fruit bat Eidolon helvum. PLoS One 6:e28131. https://doi.org/10.1371/journal.pone.0028131.
32. Hoenen T, Shabman RS, Groseth A, Herwig A, Weber M, Schudt G, Dolnik O, Basler CF, Becker S, Feldmann H. 2012. Inclusion bodies are a site of ebolavirus replication. J Virol 86:11779–11788. https://doi.org/10.1128/JVI.01525-12.
33. Neumann G, Feldmann H, Watanabe S, Lukashevich I, Kawaoka Y. 2002. Reverse genetics demonstrates that proteolytic processing of the Ebola virus glycoprotein is not essential for replication in cell culture. J Virol 76:406–410. https://doi.org/10.1128/JVI.76.1.406-410.2002.
34. Paijo J, Doring M, Spanier J, Grabski E, Nooruzzaman M, Schmidt T, Witte G, Messerle M, Hornung V, Kaever V, Kalinke U. 2016. cGAS senses human cytomegalovirus and induces type I interferon responses in human monocyte-derived cells. PLoS Pathog 12:e1005546. https://doi.org/10.1371/journal.ppat.1005546.
35. Hoffmann M, Kruger N, Zmora P, Wrensch F, Herrler G, Pöhlmann S. 2016. The hemagglutinin of bat-associated influenza viruses is activated by TMPRSS2 for pH-dependent entry into bat but not human cells. PLoS One 11:e0152134. https://doi.org/10.1371/journal.pone.0152134.